State Variables of the Arm May Be Encoded by Single Neuron Activity in the Monkey Motor Cortex

Eizo Miyashita, *Memeber, IEEE* and Yutaka Sakaguchi

***Abstract*—Revealing the type of information encoded by neurons activity in the motor cortex is essential not only for understanding the mechanism of motion control but also for developing a brain-machine interface. Thus far, the concept of preferred direction vector (PD) has dominated the discussion regarding how neural activity encodes information; however, a unified view of exactly what information is encoded has not yet been established. In the present study, a model was constructed to describe temporal neuron activity by a dot product of the PD and the movement variables vector consisting of joint torque and angular velocity. The plausibility of this model was tested by comparing estimated neural activity with that recorded from the monkey motor cortex, and it was found that this model was able to explain the temporal pattern of neuron activity irrespective of its passive responsiveness. The mean determination coefficients of neurons that responded to proprioceptive stimuli and that responded to visual stimuli were relatively high values of 0.57 and 0.58, respectively. These results suggest that neurons in the monkey motor cortex encode state variables of the arm in a framework of modern control theory and that this information could be decoded for controlling a brain-machine interface.**

***Index Terms*—Biological system modeling, computational systems biology, neural engineering, neural prosthesis**

I. Introduction

Decoding information from brain activity has been established as a theme of engineering, and the decoded information is expected to be utilized so as to develop assistive devices, e.g. brain-machine interface [1]. Brain science has focused on understanding representation or encoding of information by brain activity, especially neural activity. In the motor cortex, which sends information to muscles through the spinal cord, the concept of preferred direction vector (PD), or a cosine-tuning function of a neuron, sparked rich discussion regarding the manner in which a single neuron encodes information [2]. Although the original PD was defined in a two-dimensional space of hand movement direction, PD can be generally defined as a vector in an arbitrary space composed of arm movement-related time-varying variables to describe a neuron's tuning properties with respect to those variables. Churchland and Shenoy [3] successfully demonstrated that the temporal firing pattern could be estimated from kinematic variables and the PD. The term PD was used in this paper to refer to the generalized meaning. So far, two different types of variables have been adopted as the ones defining PD depending on task conditions.

Evidence indicates that neuron activity in the motor cortex under isotonic task conditions represents kinetic variables [4-7]. However, Georgopoulos et al. [2, 8] originally defined the PD of time-averaged neural activity for hand movement direction using Cartesian coordinates. In this line, a population vector of PDs of instantaneous neural activity was considered to represent hand movement velocity in Cartesian coordinates [9, 10]. Under isometric conditions, on the other hand, it has been defined for variables related to statics in Cartesian coordinates [11, 12] or joint angle coordinates [13, 14] (e.g., hand force or joint torque, respectively).

In the present study, the variables were focused on, not the coordinate system. However, a coordinate system is essential to define the variables [15]. Theoretical [16] and numerical simulation studies [17] have demonstrated that the hypothetical representation of muscle length on neural activity can reproduce characteristics of hand movement direction PD. Kakei et al. [18] demonstrated experimentally that the PD of time-averaged neural activity was correlated with that of time-averaged muscular activity during wrist movements. Other researchers [19, 20] have also argued that neural activity in the motor cortex represents information in joint coordinates but not in Cartesian coordinates. They claim that only a representation in joint coordinates would be able to explain the finding that, despite similar hand movement directions and distances in Cartesian coordinates, neural PDs shifted systematically with initial hand position [21, 22]. Hand force PD under isometric conditions was also reported to be dependent on posture or the starting position of the hand [23, 24]. These posture-dependent shifts of PD could be theoretically defined as a function of an intrinsic coordinate

Manuscript received April 28, 2015. This work was supported in part by the Japanese Ministry of Education, Culture, Sports, Science, and Technology under Grant-in-Aid for Young Scientists (09780773) and Grant-in-Aid for Scientific Research on Innovative Areas, "The study on the neural dynamics for understanding communication in terms of complex hetero systems (No. 4103)" (211200112)

E. Miyashita is with the Department of Computational Intelligence and Systems Science, Tokyo Institute of Technology, Yokohama 226-8502 Japan on leave from the National Institute for Physiological Sciences, Okazaki Japan (phone: +81-45-924-5573; fax: +81-45-924-5681; e-mail: miyashita.e.aa@m.titech.ac.jp).

Y. Sakaguchi is with the Department of Human Media Systems, University of Electro-Communications, Chofu 182-8585 Japan (e-mail: sakaguchi@is.uec.ac.jp).

system [25]. Thus, representation in intrinsic coordinates (e.g., muscle or joint coordinates) appears to be more consistent than that in extrinsic coordinates (e.g., Cartesian coordinates). However, one report refuted the idea of single coordinate system representation in the motor cortex [26]. According to the evidence and measurability of the movement variables, joint coordinates was adopted as the coordinate system in which PD was defined in the present study.

To formulate an information representation framework that systematically explains previous findings irrespective of the task conditions, the following formula was proposed as a model:

$$F(t+\alpha) = \mathbf{PD} \bullet \mathbf{M}^{\mathrm{T}}(t) + c = \mathbf{PD}_{\tau} \bullet \mathbf{T}^{\mathrm{T}}(t) + \mathbf{PD}_{\dot{\theta}} \bullet \dot{\mathbf{\Theta}}^{\mathrm{T}}(t) + c \,, \qquad (1)$$

where $F(t)$ is an instantaneous firing rate of a neuron at time t, α is lag time, **PD** is a vector of PD, $\mathbf{M}(t)$ is a vector of variables composed of joint torque and joint angular velocity at time t, and c is a constant. $\mathbf{PD}_{\tau}$ and $\mathbf{PD}_{\dot{\theta}}$ are component vectors of **PD** corresponding to joint torque and joint angular velocity, respectively, and $\mathbf{T}(t)$ and $\dot{\mathbf{\Theta}}(t)$ are vectors of joint torque and joint angular velocity at time t, respectively. To minimize the number of variables and to reduce multicollinearity among the variables, the joint torque and angular velocity were adopted as a kinetic or static variable and a kinematic variable, respectively, both of which have been reported to correlate with neural activity of the motor cortex [1-13]. Based on this model, five sub-models were constructed: one bidirectional model, in which a common variable represents both flexion and extension directional variables of a joint movement, and four unidirectional models, in which flexion and extension movements were treated as separate variables. In this way, it can be assumed that the bidirectional model corresponds to a neuron correlated with net torque and bidirectional angular velocity, and the unidirectional model corresponds to a neuron correlated with torque and angular velocity of flexion or extension direction at each joint. To test the validity of this model, measured neural activity in the motor cortex was compared with activity estimated by this model under an isotonic condition using both joint torque and joint angular velocity as explanatory variables. The present study is an extension of a preliminary study [27]; data analysis was applied to neurons that had passive responsiveness to visual stimuli in addition to proprioceptive stimuli.

II. Materials and Methods

A. Animal subjects and surgical procedures

Two 7.2–7.8-kg Japanese monkeys (*Macaca fuscata*) were used. A surgical operation was performed under aseptic conditions while monitoring heart rate and blood saturated oxygen concentration. The monkey was deeply anesthetized with pentobarbital (40 mg/kg, i.v. for an initial dose; 20 mg/kg, i.v. for a supplementary dose) during the surgical procedure. After the skull over the motor cortex had been removed, a recording chamber and a head holder were installed on the monkey skull and fixed with dental cement (Shohu, Kyoto, Japan). All procedures for animal care and experimental protocols were in accordance with the National Institutes of Health *Guide for the Care and Use of Laboratory Animals* and were approved by the Animal Experimentation Committee of the National Institute for Physiological Sciences.

B. General setup

The monkey sat comfortably in a primate chair with his head fixed. A digitizing tablet was placed horizontally in front of his body at chest level. The central 30 cm × 30 cm area of the tablet served as a working surface over which the monkey moved a handle of a two-joint manipulandum grasped with his hand in a pronated position. No restrictions were imposed on the performing hand's movements; the other hand was loosely restrained.

With technical limitations, the position of the handle was detected by two different measuring systems [Fig. 1(a)]. In one system, a coil was attached to the handle of the manipulandum and its position was detected by use of the digitizing tablet (Wacom, Saitama, Japan) with a sampling rate of 100 Hz. This information was utilized to display the hand position as a cursor on a CRT monitor (size: 17 inches; refresh rate: 75 Hz) (Totoku, Tokyo, Japan). In the other system, two infrared light-emitting diodes (LEDs) were placed on a distal shaft, 100 mm and 150 mm apart from the handle, and positions were measured by a position-sensitive device camera (Hamamatsu Photonics, Shizuoka, Japan) at a sampling rate of 300 Hz. This information was transformed into the position of the handle or hand of the monkey using the length of his forearm and upper arm (measured with three additional LEDs attached to his elbow and both shoulder joints, which were removed during the recording sessions).

Targets for a movement and the current hand position were displayed on the CRT monitor, which was approximately 41 cm away at the monkey's eye level. Eight potential circular targets were placed in a concentric circle surrounding a home point in a clockwise direction (i.e., 0°, 45°, 90°, 135°, 180°, 225°, 270°, and 315°; Fig. 1(a), top). Diameters of the home and target were 24 mm and the distance from the home to a target was 95 mm. The current hand position was represented as a cursor, which was a circle with a diameter of 11 mm.

C. Behavioral task

The monkey had to bring the cursor to the home or one of targets on the screen by moving the handle of the manipulandum with his hand. The sequence of a trial was as follows [Fig. 1(b)]: 1) the home appeared, indicating the start of a trial, 2) the monkey had to move the cursor onto the home and keep it within the home circle for a random period of time (0.5–1.0 s), 3) a target appeared immediately after the home disappeared, 4) the monkey had to move over the target within a second, 5) a reward was provided if he successfully hit the target. One second was chosen for the monkey to move its hand at natural speed without any rash. The task was performed in a block. One block consisted of eight successful trials in which the monkey hit all eight different targets in a

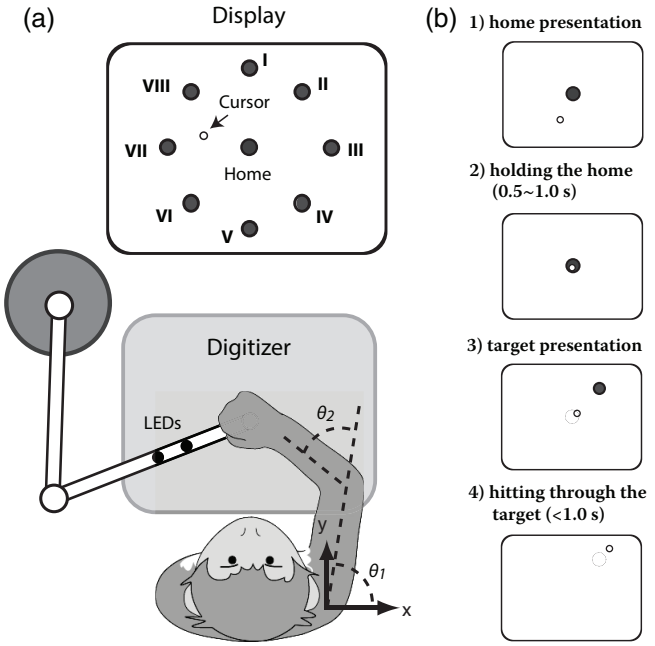

Fig. 1. Setup of the experiment and sequence of the behavioral task. (a) The monkey was required to move the handle of a passive two-joint manipulandum. The monkey's hand position was estimated from the positions of two infrared LEDs attached to the distal shaft of the manipulandum. Handle position was represented by a cursor on a CRT monitor. (b) The temporal sequence of the task was as follows: 1) the home appeared, 2) the monkey kept the cursor within the home circle for 0.5–1.0 s, 3) the home disappeared and one of the eight targets appeared, and 4) the monkey had to hit the target with the cursor within 1 s.

pseudorandom sequence. The monkey had to perform 12 blocks in a session. Prior to recording neural activity, the monkey was well trained to perform this task so as to reduce variance among each trial.

A *pass through* task was adopted instead of a *reach and hold* task. That is, the monkey was not required to hold the cursor position within the target circle at the end of the movement. One reason was to minimize feedback control elements and to focus on analysis of feed-forward control elements of neural activity. Another reason was to minimize change of muscle activity related to co-contraction during the arm movement. Since the net torque of each joint was explicitly implemented into the present model as explanatory variables, the change in co-contraction level during the task could cause undesirable effects on the model plausibility test. A previous study demonstrated that agonist and antagonist muscle co-contraction strength increased as the target size was decreased in the reach and hold task [28] suggesting that the precision required near the target increased stiffness around the arm joints. These effects were detrimental for our purposes. Adopting the *pass through* task was expected to reduce such undesirable effects.

D. Online recording and off-line analysis of data

The recording session of neural activity started after a week of recovery following surgery. A handmade glass-coated Elgiloy electrode (1.0–1.5 MΩ impedance for 1 kHz pulse passage with the electrode tip dipped in a saline) was used for recording. A glass capillary was used as a guide tube to place the electrode in a precise location over the cerebral cortex. The glass capillary with the electrode was placed on the surface of the dura using a manipulator attached to the recording chamber.

Neural activity and the positions of two LEDs were recorded with a data recorder (TEAC, Tokyo, Japan) for off-line data analysis. Neural activity in the motor cortex was systematically recorded with 1-mm grids through a glass-coated Elgiloy electrode with high-pass filter at 300 Hz and low-pass filter at 10,000 Hz.

Recorded neural activity was digitized at a sampling rate of 40 kHz. First, spike activity was detected when the amplitude exceded or fell below a threshold level, which was spike-firing timing, and data of 0.25 ms before and 0.75 ms after this timing was treated as a spike. Because these spikes consist of multiple neurons activity, then, spike-sorting was performed using custom software programmed with LabView (National Instruments, Austin, TX) to isolate single neuron activity. Specifically, cluster cutting was applied in a two-dimensional feature space of the spike interval and amplitude (i.e., either peak-to-valley or valley-to-peak) of the spike. The peak and valley were estimated by applying quadratic curve fitting on the spik. Spike-firing timing of each neuron was collected for calculation of trial-averaged spike-firing frequency.

On the other hand, recorded LEDs' positions were sampled at a rate of 1 kHz and translated to the monkey's hand position in Cartesian coordinates. A moving average filter with a 40-ms time window was applied to the hand position to smooth the signal enough to calculate its derivatives (i.e., hand velocity and acceleration).

After the recording session, passive responsiveness of the neural activity was tested applying stimuli by expeimenter's hand and monitoring sound of the neural activity. Tactile stimuli were applied by touching or stroking the skin. Proprioceptive stimuli were applied by passive movement around joints or maneuver manipulation of muscles. Visual stimulation was applied by moving experimenter's hand in front of the monkey. Each stimulation was applied at least 5 times to confirm consistency of the passive responsiveness, which was determined based on the change of pitch of monitored sound of the neural activity.

E. Calculating arm kinematics

Shoulder (θ_1) and elbow (θ_2) joint angles were calculated from the hand position using the following equations:

$$\theta_1 = \tan^{-1}\left(\frac{y}{x}\right) - \cos^{-1}\left(\frac{l_1^2 - l_2^2 + x^2 + y^2}{2l_1\sqrt{x^2+y^2}}\right) \quad (2)$$

$$\theta_2 = -\cos^{-1}\left(\frac{l_1^2 + l_2^2 - x^2 - y^2}{2l_1 l_2}\right), \quad (3)$$

where x and y are the x- and y-axis elements of the hand position in Cartesian coordinates [Fig.1(a)], respectively, and l_1 and l_2 are the upper arm and forearm lengths, respectively.

Angular velocity and acceleration of each joint angle were calculated by numerically differentiating the corresponding joint angles.

F. Calculating arm dynamics

Weight and center of gravity of the forearm (including the hand) and the upper arm were measured after the experiment. Forearm inertia moments around the elbow joint and the upper arm around the shoulder were estimated by regarding them as cylinders. Total torque necessary to achieve hand kinematics were determined as follows: 1) calculating the joint torque necessary for moving the monkey arm, 2) calculating the force necessary to move the manipulandum, and 3) calculating the total joint torque.

First, monkey arm dynamics were determined in both Cartesian and joint angle coordinate systems. Joint torque was calculated by the following equation:

$$\mathbf{T}_A = \mathbf{M}_A(\mathbf{\Theta}_A)\ddot{\mathbf{\Theta}}_A + \mathbf{V}_A(\mathbf{\Theta}_A, \dot{\mathbf{\Theta}}_A) \tag{4}$$

$$\mathbf{T}_A = \begin{bmatrix} \tau_1 \\ \tau_2 \end{bmatrix}, \ \mathbf{\Theta}_A = \begin{bmatrix} \theta_1 \\ \theta_2 \end{bmatrix} \tag{5}$$

$$\mathbf{M}_A(\mathbf{\Theta}_A) = \begin{bmatrix} I_1 + I_2 + 2m_2 l_1 l_{g2} \cos\theta_2 + m_2 l_1^2 & I_2 + m_2 l_1 l_{g2} \cos\theta_2 \\ I_2 + m_2 l_1 l_{g2} \cos\theta_2 & I_2 \end{bmatrix} \tag{6}$$

$$\mathbf{V}_A(\mathbf{\Theta}_A, \dot{\mathbf{\Theta}}_A) = \begin{bmatrix} -m_2 l_1 l_{g2} \sin\theta_2 \left(2\dot{\theta}_1\dot{\theta}_2 + \ddot{\theta}_2\right) \\ m_2 l_1 l_{g2} \dot{\theta}_2^2 \sin\theta_2 \end{bmatrix}, \tag{7}$$

where τ_1 and τ_2 are the shoulder and elbow joint torques, respectively, and I_1 and I_2 are inertia moments of the upper arm around the shoulder joint and the forearm around the elbow joint, respectively, and m_2 and l_{g2} are the weight of the forearm and distance from the elbow joint to the center of gravity of the forearm, respectively. The first and second terms on the right side of (4) correspond to inertial force and Coriolis and centrifugal forces, respectively.

Second, the dynamics of the manipulandum were calculated in the same manner and through an appropriate coordinate transformation. The following equation was obtained:

$$\mathbf{F}_M = \mathbf{M}_M(\mathbf{\Theta}_M)\ddot{\mathbf{X}} + \mathbf{V}_M(\mathbf{\Theta}_M, \dot{\mathbf{\Theta}}_M), \tag{8}$$

where $\mathbf{F}_M$ and $\ddot{\mathbf{X}}$ are a force vector to move the manipulandum and an acceleration vector of the hand, respectively. The first and second terms on the right side of the equation correspond to inertial force and Coriolis and centrifugal forces, respectively. Finally, the total torque vector ($\mathbf{T}$) required to move both of the arms and manipulandum was calculated from (4) and (8) as follows:

$$\mathbf{T} = \mathbf{T}_A + \mathbf{J}^{\mathrm{T}}(\mathbf{\Theta}_A)\mathbf{F}_M = \mathbf{M}(\mathbf{\Theta})\ddot{\mathbf{\Theta}}_A + \mathbf{V}(\mathbf{\Theta}, \dot{\mathbf{\Theta}}) \tag{9}$$

$$\mathbf{M}(\mathbf{\Theta}) = \mathbf{M}_A(\mathbf{\Theta}_A) + \mathbf{J}^{\mathrm{T}}(\mathbf{\Theta}_A)\mathbf{M}_M(\mathbf{\Theta}_M) \tag{10}$$

$$\mathbf{V}(\mathbf{\Theta}, \dot{\mathbf{\Theta}}) = \mathbf{V}_A(\mathbf{\Theta}_A, \dot{\mathbf{\Theta}}_A) + \mathbf{J}^{\mathrm{T}}(\mathbf{\Theta}_A)\mathbf{V}_M(\mathbf{\Theta}_M, \dot{\mathbf{\Theta}}_M), \tag{11}$$

where $\mathbf{J}^{\mathrm{T}}(\mathbf{\Theta}_A)$ is the transpose Jacobian of the relationship between joint angles and manipulandum position. The total torque of each joint was used for the analysis.

G. Calculating the trial-averaged spike-firing rate

Data of spike-firing timing was aligned upon movement onset, which was defined in this paper as the time when tangential acceleration of the hand was equal to or greater than 1.3 m/s^2. Trial-averaged spike-firing rates for eight different targets were calculated using a 1-ms interval. After applying the moving average with a 40 ms time window, the data were resampled at a 10-ms interval. The data from 400 ms before movement onset to 400 ms after movement onset were used for the analysis.

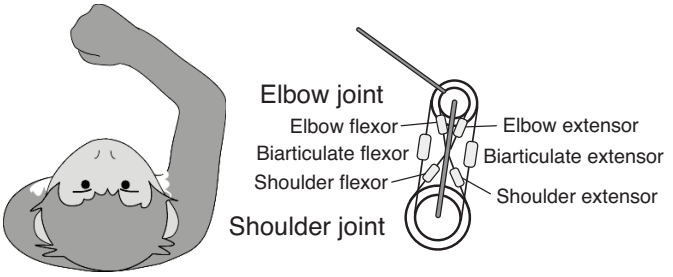

Fig. 2. Musculoskeletal system of the arm simplified as a 2-joint and 6-muscle model. Single joint (2 flexors and extensors) and biarticulate (1 flexor and extensor) muscles drive the shoulder and elbow joints. Flexor and extensor muscles generate flexion and extension torques, respectively.

H. Determining PDs using multiple linear regression analysis

A model to explain the temporal spike-firing rate of a single neuron was constructed as follows:

$$F(t+\alpha) = \mathbf{PD} \bullet \mathbf{M}(t) + c = \mathbf{PD}_\tau \bullet \mathbf{T}(t) + \mathbf{PD}_{\dot{\theta}} \bullet \dot{\mathbf{\Theta}}(t) + c \tag{12}$$

$$= a_s \times \tau_s(t) + a_e \times \tau_e(t) + b_s \times \dot{\theta}_1(t) + b_e \times \dot{\theta}_2(t) + c \tag{13}$$

where $F(t)$ is an instantaneous firing rate of a neuron at time t, α is lag time, **PD** is a row vector of PD, $\mathbf{M}(t)$ is column vector of movement variables composed of joint torque and joint angular velocity at time t, and c is a constant. $\mathbf{PD}_\tau$ and $\mathbf{PD}_{\dot{\theta}}$ are component vectors of **PD** corresponding to joint torque and joint angular velocity, respectively. $\tau_s(t)$ and $\tau_e(t)$ are total torques of the shoulder and elbow joint at time t, respectively, and $\dot{\theta}_1(t)$ and $\dot{\theta}_2(t)$ are angular velocities of the shoulder and elbow joints at time t, respectively. Here, bidirectional and unidirectional models were constructed and the plausibility was tested. In the bidirectional model, each explanatory variable explained both flexion and extension movements around the joint, representing both positive and negative values. This is a conventional model supposing that actuators of the joints are like electric motors, in which a net torque is controlled. In the unidirectional model, each explanatory variable explained only one of the flexion and extension movements selectively. The rationale of this model originate in a biomechanical structure of the arm. Musculoskeletal system of the arm can be considered as a control object consisting of 2 joints and 6 muscles; each muscle generates flexion or extension torque around the shoulder and/or elbow joints [Fig. 2]. The net torque is represented as a difference of the flexion and extension torques.

In the unidirectional model, the following were used as flexion-selective explanatory variables:

$$\tau_\gamma(t) = \begin{cases} \tau_\gamma(t) & \text{if } \tau_\gamma(t) > 0 \\ 0 & \text{otherwise} \end{cases} \quad (\gamma = s \text{ or } e) \tag{14}$$

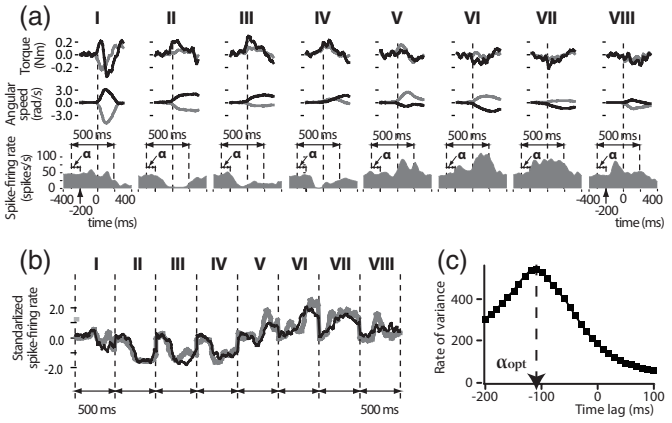

Fig. 3. Standardized regression analysis. (a) Inter-trial average firing rate of a neuron, joint torque, and angular velocity were calculated and aligned on movement onset for eight different targets (I–VIII). The black and gray lines indicate shoulder and elbow movement variables, respectively. (b) Inter-trial firing rate average was collected for eight movement directions within a time range from –200 + α ms to 300 + α ms, with lag time α, and combined into serial data with a length of 4 s (gray line). In the same way, the data from each explanatory variable were collected within a range of time from –200 ms to 300 ms and combined into serial data. After standardizing all of these variables, the explanatory variables were regressed on the inter-trial average firing rate, and the variance rate was calculated. The black line indicated estimated firing rate using an optimal lag time (α). (c) The optimal α for a neuron.was obtained so that the variance rate was maximum, which means that the estimation error was minimum.

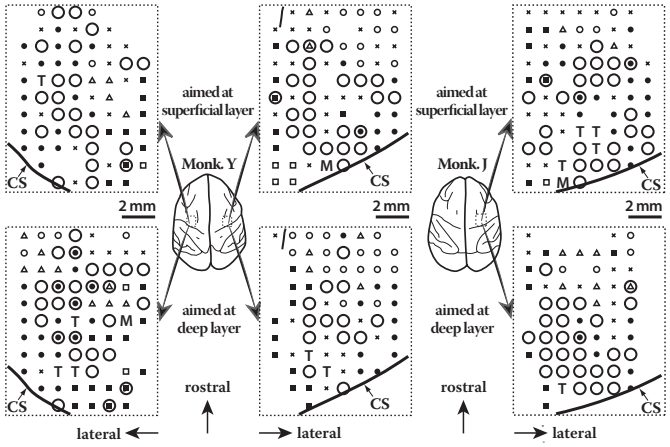

Fig. 4. Recording sites and passive responsiveness of recorded neural activity. Electrode placement was aimed at both superficial and deep layers of the cerebral cortex. The central sulcus is abbreviated as CS. The types of passive responsiveness are symbolized as follows: maneuver manipulation of the pectoralis major, biceps, or triceps (M), touch on the skin surface of the forearm and/or upper arm (T), passive movement of the shoulder and/or elbow joints (large open circle), passive movement of the wrist and/or digit joints or touch on the skin surface of the hand (small closed circle), body axis rotation or touch on the skin surface of the back (small closed square), touch on the skin surface of the head and/or neck (small open square), visual stimulus (small open triangle), and no obvious response (small cross). Neural activity responded to spontaneous arm movements without obvious passive responsiveness is also indicated as a small open circle.

$$\dot{\theta}_{\beta}(t)=\begin{cases}\dot{\theta}_{\beta}(t) & \text{if } \dot{\theta}_{\beta}(t)>0\\ 0 & \text{otherwise}\end{cases}\quad(\beta=1 \text{ or } 2)\,. \tag{15}$$

For the extension-selective variables, the following were used as explanatory variables:

$$\tau_{\gamma}(t)=\begin{cases}\tau_{\gamma}(t) & \text{if } \tau_{\gamma}(t)<0\\ 0 & \text{otherwise}\end{cases}\quad(\gamma=s \text{ or } e) \tag{16}$$

$$\dot{\theta}_{\beta}(t)=\begin{cases}\dot{\theta}_{\beta}(t) & \text{if } \dot{\theta}_{\beta}(t)<0\\ 0 & \text{otherwise}\end{cases}\quad(\beta=1 \text{ or } 2)\,. \tag{17}$$

One directional selectivity was assigend to each joint, and thereby four types of unidirectional models (shoulder, elbow) = [flexion selective (+), flexion selective (+)], [flexion (+), extension (–)], [extension (–), flexion (+)], and [extension (–), extension (–)] were obtained.

Standardized multiple linear regression analysis was used to compare the contribution of each explanatory variable to the variability of the firing rate of a neuron. The data for each explanatory variable was collected for eight movement directions within a range of time from –200 to 300 ms, with the movement onset defined as time zero. The data for eight directions were combined into a serial data set with a length of 4 s for each variable. These 4-s joint torque and angular velocity data sets were standardized and used for the regression analysis [Fig. 3(a)].

In the same manner, trial-averaged spike-firing rate data for eight movement directions were collected within a range of time from –200 + α ms to 300 + α ms, with time lag α (–200 ms $\le \alpha \le$ 100 ms) [Fig. 3(a)]. Data for eight targets were combined into a serial data set with a length of 4 s. These 4-s data sets of the trial-averaged spike-firing rate were standardized and regressed on the explanatory variable with a constant bias [Fig. 3(b)].

First, the optimal time lag α that maximize the variance rate, in other words, that minimizes approximation error was obtained [Fig. 3(c)]. Then, the coefficient of determination (R^2) and regression coefficients with that optimal time lag was obtained as the representative value for a given model. Neuronal joint torque and angular velocity PDs were defined as vectors $\mathbf{PD}_{\tau}=(a_s,a_e)$ and $\mathbf{PD}_{\theta}=(b_s,b_e)$, respectively. To quantify a contribution ratio of each variable to the variability of a neural activity, the PD gain-ratio was defined as $\|\mathbf{PD}_{\tau}\|/\|\mathbf{PD}_{\theta}\|$.

III. Results

A. Recording sites and passive responsiveness

Neural activity was recorded from three hemispheres of two monkeys. All recordings were done from the contralateral motor cortex to the performing arm. Penetrations of the electorode were systematically made at 1-mm intervals for both superficial and deep layers of the cerebral cortex [Fig. 4]. At recording sites up to 5–7 mm rostral to the central sulcus of the cerebral cortex, most of the arm movement-related neurons responded to passive movements of the shoulder and/or elbow joints, while some responded to touch on the arm skin surface. Maneuver manipulation of arm-controlling muscles elicited neural activity at only a few recording sites. In this region, parts of the body that elicited the neural responses were roughly somatotopically represented in the mediolateral

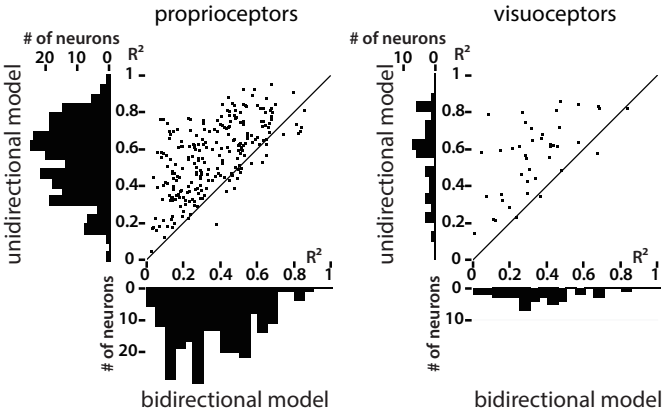

Fig. 5. Comparisons of goodness of fit for *proprioceptors* and *visuoceptors*; the unidirectional versus bidirectional models. Each dot in scatterplots represents the coefficient of determinant (R^2) of a neuron when spike-firing rate of it was forced to fit with either directional model. The values of the bidirectional and unidirectional models were represented on horizontal- and vertical- axes, respectively. The distributions of R^2 for each model was also showed as histograms.

direction on the brain surface (i.e., from the shoulder to the digits). At recording sites more than 5–7 mm rostral to the central sulcus, neurons predominantly responded to visual stimuli or to spontaneous arm movements without obvious passive responsiveness. These tendencies were consistent through different depths, hemispheres, and individuals.

A multiple regression analysis was applied only to the neurons that were located rostral to the central sulcus and that responded to proprioceptive stimuli (passive movements of the shoulder and/or elbow joints or maneuver manipulations of the muscles controlling the joints) and/or to visual stimuli. Neurons were classified into two types in this paper depending on their responsiveness to stimuli: *proprioceptors* and *visuoceptors*. The *proprioceptors* were defined as neurons that responded to proprioceptive stimuli with or without responsiveness to visual stimuli. The *visuoceptors* were defined as neurons that responded to visual stimuli without responsiveness to proprioceptive stimuli. As a result, 241 *proprioceptors* (99 and 60 neurons from the left and right hemispheres of monkey Y, respectively, and 82 neurons from the right hemisphere of monkey J) recorded from 138 electrode penetration sites and 42 *visuoceptors* (21 and seven neurons from the left and right hemispheres of monkey Y, respectively, and 14 neurons from the right hemisphere of monkey J) recorded from 24 electrode penetration sites were used for the regression analysis. Because of the technical limitation to identify the type of passive responsiveness of the neurons, the number of the *visuoceptors* might be underestimated.

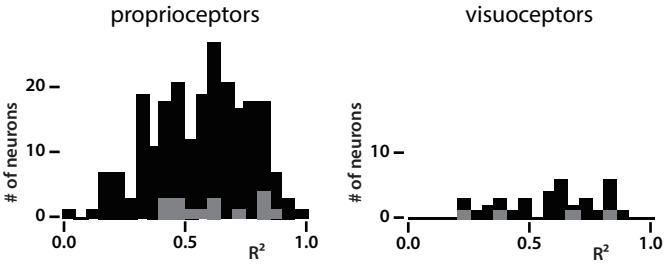

Fig. 6. Distribution histograms of the determination coefficient (R^2) of the best model for *proprioceptors* and *visuoceptors*. Black and gray bars indicate neurons best fit by the unidirectional and bidirectional models, respectively.

B. Goodness of fit

Standardized regression analysis was applied to 241 *proprioceptors* and 42 *visuoceptors* for five models (i.e., a bidirectional and four unidirectional). When either directional model (i.e., unidirectional or bidirectional) was forced, the unidirectional model fit (the best-fitting model among the four sub-models; $R^2 = 0.56 \pm 0.19$ and 0.56 ± 0.20 for the *proprioceptors* and *visuoceptors*, respectively) was much better than the fit of the bidirectional model ($R^2 = 0.36 \pm 0.20$ and 0.34 ± 0.19 for the *proprioceptors* and *visuoceptors*, respectively) [Fig. 5]. Of these neurons, 10 *proprioceptors* and six *visuoceptors* had a lag time α outside the range of –200 ms $< \alpha <$ 100 ms for all the models. This meant either that the neurons were less likely to be correlated with ongoing movements or that the explanatory variables were inappropriate. Therefore, these 10 *proprioceptors* and six *visuoceptors* were excluded from further analyses.

The best fit for the majority of *proprioceptors* (93%; 214/231) and *visuoceptors* (89%; 32/36) was accomplished by the unidirectional model, with an R^2 equal to 0.56 ± 0.19 and 0.58 ± 0.19 (mean ± SD) , respectively [Fig. 6, black bars]. Regarding the sub-models of the unidirectional neurons, 64, 51, 41, and 58 *proprioceptors* and eight, nine, four, and 11 *visuoceptors* were best fit by the (+, +), (+, –), (–, +), and (–, –) models, respectively. The remaining 17 *proprioceptors* (7%) and four *visuoceptors* (11%) were best fit by the bidirectional model, with R^2 equal to 0.63 ± 0.16 and 0.53 ± 0.28 (mean ± SD), respectively [Fig. 6, gray bars]. The overall

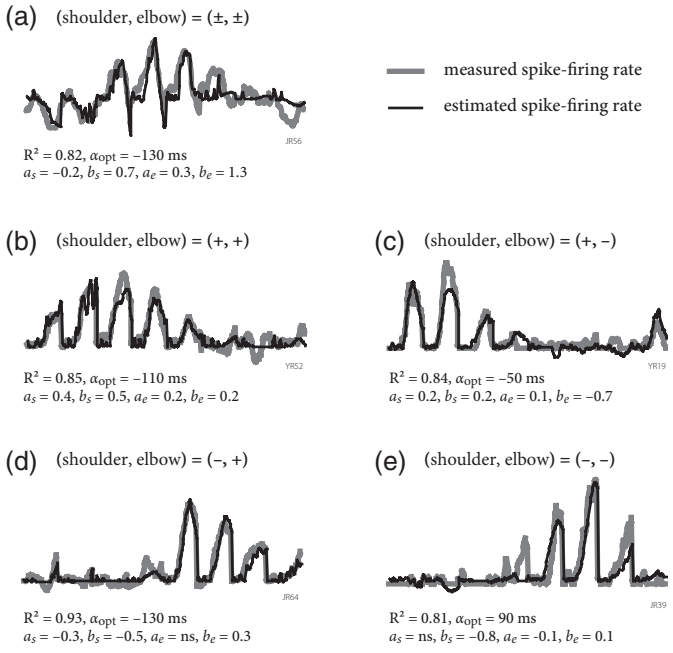

Fig. 7. Examples of each neuron best fit by each type of the models. Spike-firing rate (gray thick lines) was fairly well approximated by the models (black lines) using bidirectional explanatory variables (a) and unidirectional explanatory variables (b), (c), and (d). Flexional and extensional direction variables were represented as + and –, respectively.

R^2 of the best model of the *proprioceptors* and *visuoceptors* was 0.57 ± 0.19 and 0.58 ± 0.20 (mean ± SD), respectively.

As for the best model, about 13% (29/231) of the *proprioceptors* and 7% (8/36) of the *visuoceptors* had an R^2 value greater than 0.8. When the temporal pattern of these neural activity was compared with the estimated activity, each model type showed surprisingly good fit in almost all movement directions [Fig. 7].

C. Neural activity lag time in relation to movement onset

The best-fit model lag times of the *proprioceptors* and *visuoceptors* were –66 ± 68 ms and –75 ± 59 (α; mean ± SD), respectively [Fig. 8]. Approximately 82% (190/231) of the *proprioceptors* and 83% (30/36) of the *visuoceptors* had a negative lag time, which indicates that neural activity preceded arm movement. The mean lag times of these *proprioceptors* and *visuoceptors* ($\alpha < 0$) were –89 ms and –96 ms, respectively.

D. PD and its gain-ratio distribution

Joint torque PD and angular velocity PD of the best model were distributed throughout four quadrants in the joint coordinates. As for joint torque PD of the *proprioceptors*, 65 (32), 45 (18), 64 (32), and 57 (13) were within the first, second, third, and fourth quadrant, respectively. The *visuoceptors* had values of 9 (4), 6 (4), 11 (4), and 10 (4), respectively. The angular velocity PD of the *proprioceptors* was 75 (12), 42 (16), 63 (14), and 51 (9), respectively. The values of the *visuoceptors* were 9 (1), 4 (2), 13 (5), and 10 (5), respectively. In each case, the number in parenthesis indicates the number of units that had nonsignificant ($p > 0.01$, which is a rather strict criteria) coefficients for at least one variable (or axis).

Very few units had nonsignificant coefficients in both axes. In the bidirectional model of the *proprioceptors*, only one neuron had nonsignificant coefficient of the angular velocity PD in both axes. In the bidirectional model of the *visuoceptors*, joint torque PD of one neuron and angular velocity PD of another neuron had nonsignificant coefficients in both axes. In the unidirectional model of the *proprioceptors*, joint torque PD of 8% (18/214) neurons and velocity PD of only 2% (5/214) neurons had nonsignificant coefficients in both axes. The unidirectional model of the *visuoceptors* had similar values of 13% (4/32) of joint torque PD and 3% (1/32) of angular velocity PD, with nonsignificant coefficients in both axes. This suggests that both joint torque and angular velocity are encoded by the activity of the majority of neurons regardless of their passive responsiveness.

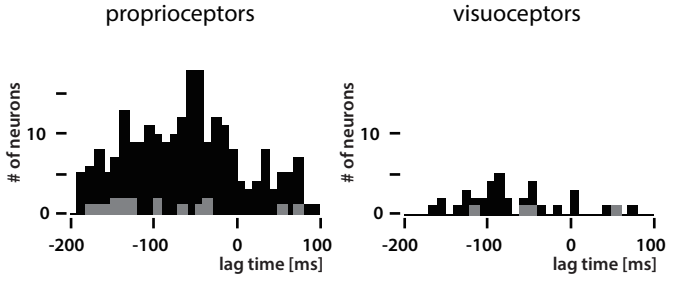

Fig. 8. Distribution histograms of the optimal lag time of the best model for *proprioceptors* and *visuoceptors*. Black and gray bars indicate neurons best fit by the unidirectional and bidirectional models, respectively.

The PD gain-ratio was distributed within the range of 1/28 to 12 and 1/19 to 5 in the *proprioceptors* and *visuoceptors*, respectively. The logarithm gain-ratio mean of the *proprioceptors* was –0.35 (the gain-ratio mean: 0.45) and that of the *visuoceptors* was similar, with a value of –0.34 (the gain-ratio mean: 0.46) [Fig. 9(a)]. This mean value was calculated by averaging all neurons, including those with nonsignificant coefficients. No significant difference ($p > 0.11$ for the *proprioceptors* and $p > 0.30$ for the *visuoceptors*, Welch's test) was observed in the logarithm mean gain-ratio between the neuron groups with nonsignificant coefficients in at least one axis and those with significant coefficients in both axes. Further examination of the relationship between the gain-ratio and the location of the neuron revealed apparent independent relationships among them [Fig. 9(b)]. No significant difference ($p > 0.42$ for the *proprioceptors* and $p > 0.75$ for the *visuoceptors*, Welch's test) was detected between the neuron groups located in the superficial layer (depth ≤1.3 mm) and those located in the deep layer (1.3 mm <depth).

IV. Discussion

A. Neural representation of movement-related variables

Information representation by neural activity in the motor cortex has been discussed in terms of PD or a cosine tuning function since Georgopoulos et al. [2, 8] introduced this idea. However, researchers have not yet established a unified view

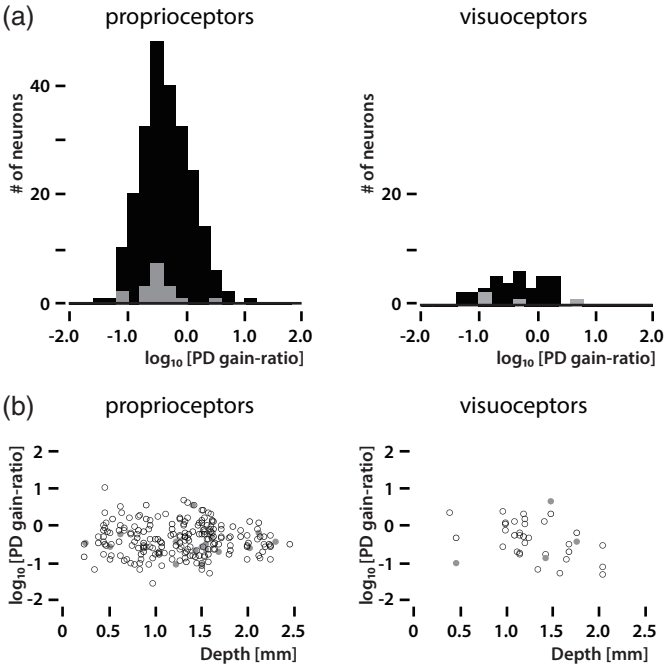

Fig. 9. (a) Distribution histograms of the logarithmic PD gain-ratio for *proprioceptors* and *visuoceptors*. Black and gray bars indicate neurons best fit by the unidirectional and bidirectional models, respectively. (b) Scatterplots of the logarithmic PD gain-ratio to the recorded location of neuron in depth of the cerebral cortex for *proprioceptors* and *visuoceptors*. Black open and gray closed circles indicate neurons best fit by the unidirectional and bidirectional models, respectively.

of what kind of information is encoded by neural activity in the motor cortex. Although kinetic or static variables (e.g., force and torque) have been used under an isometric condition [11-14, 23, 24] to explain neural activity in terms of PD, only kinematic variables (e.g., movement direction, hand position, hand velocity, hand acceleration, and combinations of these) have been used under an isotonic condition in the previous studies [2, 3, 8, 29]. To explain neural activity under two different conditions with a single model, both kinetic or static variables and kinematic variables were included into the present unified model. The present model degenerates into the conventional model with only static variables under the isometric condition, as the kinematic variables are zero under such a condition. Under an isotonic condition, however, neural activity would be characterized by both PDs of kinetic variables and of kinematic variables, as opposed to only the PD of kinematic variables as in previous studies. Recently, both kinetic and kinematic information was successfully decoded from ensembles of neuron activity in the motor cortex [30].

The results showed that joint torque and angular velocity PD gain-ratio distributed roughly from 1/30 to 10, with mean values of 0.45 and 0.46 for the *proprioceptors* and *visuoceptors*, respectively. Thus, at the population level under our condition, the contribution of angular velocity to neural activity would be two times greater than that of torque. If this relationship holds for other experimental conditions, only the velocity variable explains most neural activity, which is in accordance with the findings of Schwartz et al. [9, 10]. In addition, the model predicts that the neuronal firing rate will change when a load is applied onto the hand during the movement. This prediction is in agreement with the findings of Kalaska et al. [6, 7].

As for the coordinate system in which the movement variables were described, joint coordinates as intrinsic coordinates were adopted in the present study. The present study showed that approximately 93% of the *proprioceptors* and 89% of the *visuoceptors* were categorized in the unidirectional model, suggesting that the majority of neurons in the motor cortex encoded unidirectional (flexion–extension direction selective) information of torque and angular velocity around the joints. This might indicate another possibility of information representation in muscle coordinates, as suggested in some studies [16-18, 31].

Temporal activity of neurons in the motor cortex should represent time-varying variables of arm movements, as the brain controls the arm in a real-time fashion. A limited number of studies have dealt with time-varying variables of arm movements [29, 32]. Churchland et al. [3] recently used time-varying variables of hand kinematics to explain temporal neural activity and showed that the R^2 population mean increased from 0.39 to 0.46 when hand acceleration and position were added to the explanatory variables (i.e., in addition to hand velocity and speed; note that they dealt with velocity and speed as different variables). Our model had a markedly better-fit performance (R^2 = 0.57, *proprioceptors*; R^2 = 0.58, *visuoceptors*) than their model, in spite of fewer

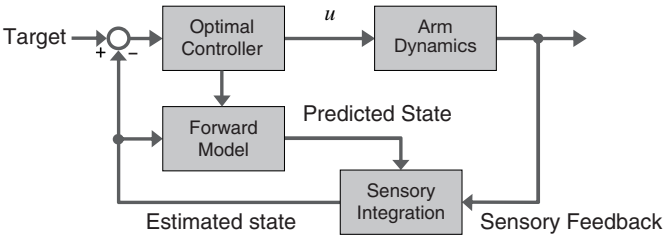

Fig. 10. Block diagram of a plausible control model of the arm movement.

explanatory variables in our model (n = 4) than in theirs (n = 7). The discrepancy may have been caused by three factors: 1) their model used Cartesian coordinates while our model used joint coordinates to describe explanatory variables, 2) theirs used hand acceleration while ours used joint torque, and 3) theirs used only bidirectional explanatory variables while ours tested both bidirectional and unidirectional variables. When joint-angle acceleration was applied instead of joint torque as an explanatory variable with our neurons, the mean R^2 of the best models of the *proprioceptors* and *visuoceptors* decreased from 0.57 to 0.53 and from 0.58 to 0.56, respectively. In contrast, the mean R^2 of the *proprioceptors* and *visuoceptors* dropped to 0.36 and 0.34, respectively, when the bidirectional model was forced to applly to all neurons. Thus, the last factor may have had a substantial effect on the discrepancy.

Using regression analysis, the present study demonstrated that the temporal activity of a single neuron in the motor cortex could be described as a dot product of a PD vector and the movement variables vector of joint torque and angular velocity as representing kinetics and kinematics, respectively. Although our model could reinterpret previous findings without any major conflicts, more concrete evidence supporting the model, especially regarding the representation of kinetic variables on the motor cortex during the movements, should try to be experimentally obtained. Since the majority neurons in the motor cortex were categorized into the unidirectional model, it is suggested that the motor cortex independently encodes information of flexion and extension torques around joints. If same amount of flexion and extension torques were produced by flexor and extensor muscles, respectively, the joint would not rotate at all since the net torque around the joint is zero, but impedance of the joint would change depending on each amount of flexion and extension torques produced at the joint. Experiments using a robotic arm manipulandum [33] and testing different impedance conditions with a similar condition of kinematics would allow us to further advance this research.

B. Arm movement control theories and neural information representation in the motor cortex

Most studies on reaching movement control theory in brain science have focused on how to reproduce behavioral characteristics, such as a bell-shaped speed profile and (slightly bent) straight hand path. Two types of models have predominated: models that explicitly require a *desired trajectory* [34-37] and those that do not [38, 39]. In the former models, a controller receives the *desired trajectory* and

generate control input so as to achieve that given trajectory using an *internal model* for inverse dynamics. In the latter models, an optimal controller receives positional information of a target and initial arm state, and then produces control input using an internal state feedback of estimated arm state, which is error-correted predicted arm state. The predicted arm state is generated by an *internal model* for forward dynamics [Fig. 10].

As far as arm kinematics is concerned, both types of the control models can reproduce characteristics of the arm movement. However, potential ability to explain characteristics of impedance of the arm is another story. The control models that explicitly require a *desired trajectory* do not inherently have the ability at all. In contrast, the control models that do not explicitly require it not only have the ability to explain characteristics of arm impedance [40, 41] but also have extensibility to explain various aspects of behavioral characteristics including adaptation to novel environments [42]. Therefore, this type of control models seems to be a plausible control model of the brain.

The present study showed that joint torque and angular velocity were represented by neural temporal activity in the motor cortex. If this finding is incorporated into the plausible control model, joint torque and angular velocity may be regarded as predicted arm state or as estimated arm state. Future experiments should be to verify which state variable is encoded by neural activity in the motor cortex.

V. Conclusion

The present study suggests that a kind of state variables of the arm is represented or encoded by neural activity in the motor cortex. This information could be decoded and be used for controlling a brain-machine interface. Further understanding of information representation in the cerebral cortex together with understanding control mechanisms of the body would contribute to developing an appropriate brain-machine interface for the brain to literally control a machine without mediating the body.

Acknowledgment

E. Miyashita would like to thank Dr. Shigemi Mori, an ex-professor of the National Institute of Physiological Science, for his generous support of the animal experiment.

References

[1] K.-K. Shyu, Y.-J. Chiu, P.-L. Lee, M.-H. Lee, J.-J. Sie, C.-H. Wu, *et al.*, "Total design of an FPGA-based brain–computer interface control hospital bed nursing system," *IEEE Trans. Ind. Electron.,* vol. 60, pp. 2731–2739, July 2013.

[2] A. P. Georgopoulos, J. F. Kalaska, R. Caminiti, and J. T. Massey, "On the relations between the direction of two-dimensional arm movements and cell discharge in primate motor cortex," *J. Neurosci.,* vol. 2, pp. 1527–1537, 1982.

[3] M. M. Churchland and K. V. Shenoy, "Temporal complexity and heterogeneity of single-neuron activity in premotor and motor cortex," *J. Neurophysiol.,* vol. 97, pp. 4235–57, Jun 2007.

[4] E. V. Evarts, "Relation of pyramidal tract activity to force exerted during voluntary movement," *J. Neurophysiol.,* vol. 31, pp. 14–27, 1968.

[5] P. D. Cheney and E. E. Fetz, "Functional classes of primate corticomotoneuronal cells and their relation to active force," *J. Neurophysiol.,* vol. 44, pp. 773–791, 1980.

[6] J. F. Kalaska, D. A. D. Cohen, M. L. Hyde, and M. Prud'homme, "A comparison of movement direction-related versus load direction-related activity in primate motor cortex, using a two-dimensional reaching task," *J. Neurosci.,* vol. 9, pp. 2080–2102, 1989.

[7] L. E. Sergio, C. Hamel-Paquet, and J. F. Kalaska, "Motor cortex neural correlates of output kinematics and kinetics during isometric-force and arm-reaching tasks," *J. Neurophysiol.,* vol. 94, pp. 2353–78, Oct 2005.

[8] A. B. Schwartz, R. E. Kettner, and A. P. Georgopoulos, "Primate motor cortex and free arm movements to visual targets in three-dimensional space. I. Relations between single cell discharge and direction of movement," *J. Neurosci.,* vol. 8, pp. 2913-27, Aug 1988.

[9] A. B. Schwartz and D. W. Moran, "Motor cortical activity during drawing movements: population representation during lemniscate tracing," *J. Neurophysiol.,* vol. 82, pp. 2705–18, Nov 1999.

[10] G. A. Reina, D. W. Moran, and A. B. Schwartz, "On the relationship between joint angular velocity and motor cortical discharge during reaching," *J. Neurophysiol.,* vol. 85, pp. 2576–89, Jun 2001.

[11] A. P. Georgopoulos, J. Ashe, N. Smyrnis, and M. Taira, "The motor cortex and the coding of force," *Science,* vol. 256, pp. 1692–1695, 1992.

[12] M. Taira, J. Boline, N. Smyrnis, A. P. Georgopoulos, and J. Ashe, "On the relations between single cell activity in the motor cortex and direction and magnitude of three-dimensional static isometric force," *Exp. Brain Res.,* vol. 109, pp. 367–376, 1996.

[13] T. M. Herter, I. Kurtzer, D. W. Cabel, K. A. Haunts, and S. H. Scott, "Characterization of torque-related activity in primary motor cortex during a multijoint postural task," *J. Neurophysiol.,* vol. 97, pp. 2887–99, Apr 2007.

[14] R. Ajemian, A. Green, D. Bullock, L. Sergio, J. Kalaska, and S. Grossberg, "Assessing the function of motor cortex: single-neuron models of how neural response is modulated by limb biomechanics," *Neuron,* vol. 58, pp. 414–28, May 8 2008.

[15] S. S. Chan and D. W. Moran, "Computational model of a primate arm: from hand position to joint angles, joint torques and muscle forces," *J. Neural Eng.,* vol. 3, pp. 327–37, Dec 2006.

[16] F. A. Mussa-Ivaldi, "Do neurons in the motor cortex encode movement direction? An alternative hypothesis," *Neurosci. Lett.,* vol. 91, pp. 106–111, 1988.

[17] E. Todorov, "Direct cortical control of muscle activation in voluntary arm movements: a model," *Nat. Neurosci.,* vol. 3, pp. 391–8, Apr 2000.

[18] S. Kakei, D. S. Hoffman, and P. L. Strick, "Muscle and movement representations in the primary motor cortex," *Science,* vol. 285, pp. 2136–9, Sep 24 1999.

[19] S. Tanaka, "Hypothetical joint-related coordinate systems in which populations of motor cortical neurons code direction of voluntary arm movements," *Neurosci. Lett.,* vol. 180, pp. 83–86, 1994.

[20] S. H. Scott and J. F. Kalaska, "Reaching movements with similar hand paths but different arm orientations. I. Activity of individual cells in motor cortex," *J. Neurophysiol.,* vol. 77, pp. 826–52, Feb 1997.

[21] R. Caminiti, P. B. Johnson, and A. Urbano, "Making arm movements within different parts of space: dynamic aspects in the primate motor cortex," *J. Neurosci.,* vol. 10, pp. 2039–2058, 1990.

[22] S. H. Scott and J. F. Kalaska, "Changes in motor cortex activity during reaching movements with similar hand paths but different arm postures," *J. Neurophysiol.,* vol. 73, pp. 2563–7, Jun 1995.

[23] L. E. Sergio and J. F. Kalaska, "Systematic changes in directional tuning of motor cortex cell activity with hand location in the workspace during generation of static isometric forces in constant spatial directions," *J. Neurophysiol.,* vol. 78, pp. 1170–4, Aug 1997.

[24] L. E. Sergio and J. F. Kalaska, "Systematic changes in motor cortex cell activity with arm posture during directional isometric force generation," *J. Neurophysiol.,* vol. 89, pp. 212–28, Jan 2003.

[25] R. Ajemian, D. Bullock, and S. Grossberg, "A model of movement coordinates in the motor cortex: posture-dependent changes in the gain and direction of single cell tuning curves," *Cereb. Cortex,* vol. 11, pp. 1124–35, Dec 2001.

[26] W. Wu and N. Hatsopoulos, "Evidence against a single coordinate system representation in the motor cortex," *Exp. Brain Res.,* vol. 175, pp. 197–210, Nov 2006.

[27] E. Miyashita and Y. Sakaguchi, "Suggestive evidence for a forward model of the arm in the monkey motor cortex," presented at the The 13th

International Workshop on Advanced Motion Control, Yokohama, Japan, pp. 191–196, 2014.
[28] P. L. Gribble, L. I. Mullin, N. Cothros, and A. Mattar, "Role of cocontraction in arm movement accuracy," *J. Neurophysiol.,* vol. 89, pp. 2396–405, May 2003.
[29] Q. G. Fu, D. Flament, J. D. Coltz, and T. J. Ebner, "Temporal encoding of movement kinematics in the discharge of primate primary motor and premotor neurons," *J. Neurophysiol.,* vol. 73, pp. 836–54, Feb 1995.
[30] A. H. Fagg, G. W. Ojakangas, L. E. Miller, and N. G. Hatsopoulos, "Kinetic trajectory decoding using motor cortical ensembles," *IEEE Trans. Neur. Sys. Reh.,* vol. 17, pp. 487–496, 2009.
[31] Y. Koike, H. Hirose, Y. Sakurai, and T. Iijima, "Prediction of arm trajectory from a small number of neuron activities in the primary motor cortex," *Neurosci. Res.,* vol. 55, pp. 146–53, Jun 2006.
[32] J. Ashe and A. P. Georgopoulos, "Movement parameters and neural activity in motor cortex and area 5," *Cereb. Cortex,* vol. 4, pp. 590–600, Nov-Dec 1994.
[33] Y. Ueyama and E. Miyashita, "Devising a robotic arm manipulandum for normal and altered reaching movements to investigate brain mechanisms of motor control," *Instru. Sci. Tech.,* vol. 41, pp. 251–273, 2013.
[34] T. Flash and N. Hogan, "The coordination of arm movements: an experimentally confined mathematical model," *J. Neurosci.,* vol. 5, pp. 1688–1703, 1985.
[35] Y. Uno, M. Kawato, and R. Suzuki, "Formation and control of optimal trajectory in human multijoint arm movement," *Biol. Cybern.,* vol. 61, pp. 89–101, 1989.
[36] M. Kawato, "Trajectory formation in arm movements: minimization principles and procedures," in *Advances in Motor Learning and Control*, H. N. Zelaznik, Ed., ed Chanpaign, Illinois: Human Kinetics Publishers, 1996, pp. 225-259.
[37] C. M. Harris and D. M. Wolpert, "Signal-dependent noise determines motor planning," *Nature,* vol. 394, pp. 780–4, Aug 20 1998.
[38] E. Todorov and M. I. Jordan, "Optimal feedback control as a theory of motor coordination," *Nat. Neurosci.,* vol. 5, pp. 1226–35, Nov 2002.
[39] W. Li and E. Todorov, "Iterative linearization methods for approximately optimal control and estimation of non-linear stochastic system," *Int. J. Control,* vol. 80, pp. 1439–1453, 2007.
[40] Y. Ueyama and E. Miyashita, "Signal-dependent noise induces muscle co-contraction to achieve required movement accuracy: a simulation study with an optimal control," *Curr. Bioinform.,* vol. 5, pp. 16–24, 2013.
[41] Y. Ueyama and E. Miyashita, "Optimal feedback control for predicting dynamic stiffness during arm movement," *IEEE Trans. Ind. Electron.,* vol. 61, pp. 1044–1052, 2014.
[42] E. Miyashita, "Toward an understanding of motion control of the body by the brain," presented at the 1st IEEJ International Workshop on Sensing, Actuation, and Motion Control, Nagoya, Japan, IS5-6, 2015.

Eizo Miyashita (M'15) received the M.D. from the Japanese Ministry of Welfare and Health in 1985 and the Ph.D. degrees from Wakayama Medical University, Wakayama, Japan in 1990.

He is currently an Associate Professor with the Department of Computational Intelligence & Systems Science, Interdisciplinary Graduate School of Science and Engineering, Tokyo Institute of Technology. His research interest includes understanding adaptive motion control mechanisms of the brain and applying the knowledge for brain-machine interface.

Yutaka Sakaguchi (M'93) received the B.E., M.E. and Ph.D. degrees from the University of Tokyo in 1986, 1988 and 1994, respectively.

He is currently a Professor with the Department of Information Media Systems, Graduate School of Information Systems, University of Electro-Communications. His research interest includes understanding of human sensorimotor system and its learning mechanism.